THE JOURNAL OF PHYSICAL CHEMISTRY Letters

Letter

pubs.acs.org/JPCL

Equivalent Circuit of Electrons and Holes in Thin Semiconductor Films for Photoelectrochemical Water Splitting Applications

Luca Bertoluzzi and Juan Bisquert*

Grup de Dispositius Fotovoltaics i Optoelectrònics, Departament de Física, Universitat Jaume I, 12071 Castelló, Spain

ABSTRACT: A simple model for the kinetics of electrons and holes in a thin semiconductor film in photoelectrochemical water splitting conditions is discussed, with a focus to discriminate between trap-assisted recombination and charge-transfer processes. We formulate the kinetic model in terms of the measurements of impedance spectroscopy and discuss the application of the results for the interpretation of the current potential curve under photogeneration. We provide a rigorous structure of the fundamental equivalent circuit for photoelectrochemical water splitting systems including a new predicted feature that is a chemical capacitance of the minority carriers that can give rise, in combination with other standard features, to a total of three arcs in the complex plane.

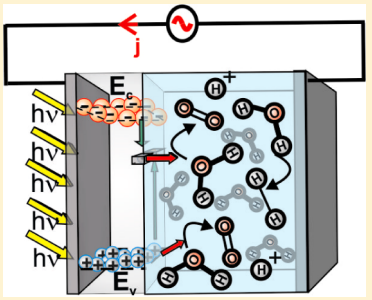

SECTION: Energy Conversion and Storage; Energy and Charge Transport

The search for stable solutions to current environmental threats has urged scientists to find an eco-friendly and sustainable source of energy. Solar energy is considered to be the best candidate because the Sun constitutes the largest abundant source of energy. One problem though is its inconstancy because of its diurnal feature, while our energy demand is permanent. Therefore, in addition to collecting and transforming the energy of the Sun, the main current preoccupation is to store it.

One attractive solution is water splitting, which allows for the storage of solar energy through chemical bonds, in this case, hydrogen molecules, as for the photosynthesis by using an appropriate semiconductor.[1−4] Although many candidate materials have been proposed, current semiconductor properties are far from being optimal. Due to several attractive features, Fe_2O_3 hematite is being intensively investigated to improve the morphology and develop new nanostructures incorporating current collectors and surface treatments with catalyst and passivation layers that would enhance the efficiency of the charge collection and reduce the onset voltage.[5−8]

It has been widely recognized that the main issues that restrain the efficiency of the water splitting process are the sluggish transfer of holes to the solution and the high recombination rate in the bulk and at the semiconductor/solution interface.[9] Even though many studies have been developed to understand the interfacial processes and particularly the recombination/charge transfer competition,[10−13] this issue remains a current subject of debate.[14−16] A number of works have recently highlighted the central role of surface traps in the kinetic operation of hematite in water splitting conditions.[17−19]

In this work, we present a simple analytical model that allows for the description of the kinetics at the interface of the semiconductor/solution at the operational voltage in order to trace the holes' recombination/charge transfer processes. An equivalent AC circuit has been established with the method of impedance spectroscopy (IS). This model reveals the presence of a possible semicircle due to the valence band capacitance and the resistance of holes charge transfer from the valence band. In the end, a brief qualitative analysis of the IS possible spectra is made as a useful tool for experimental interpretations.

A simple model is presented, describing the kinetics of carriers at the semiconductor/electrolyte interface under illumination in water splitting conditions in the presence of a level containing N_t traps at the energy E_t, as illustrated in Figure 1. In this model, a very thin layer of semiconductor of length d is considered with a metal contact at the left and a contact with electrolyte at the right boundary that permits the transference of holes both from the surface state level and from the valence band level. For simplicity, cathodic current is neglected. We write n, p, and f, respectively, as the electron density, the hole density, and the probability that an electron occupies a trap. n_0, p_0, and f_0 represent the same respective quantities at equilibrium. We assume that the electron density at the metal contact ($x = 0$) can be directly regulated by the applied voltage V.

$$n(0) = N_c \exp\left(\frac{E_{Fn} - E_c}{k_B T}\right) = n_0 \exp\left(-\frac{qV}{k_B T}\right) \quad (1)$$

In Figure 1, the voltage is referred to the redox energy in the electrolyte, but it can also be measured with respect to the reference electrode. E_c is the energy of the lower edge of the conduction band, E_{Fn} is the electron quasi Fermi level, which has the value E_{F0} at equilibrium, N_c is an effective density of states at the conduction band, and $k_B T$ is the thermal energy.

Received: August 1, 2012
Accepted: August 23, 2012

   dx.doi.org/10.1021/jz3010909 | J. Phys. Chem. Lett. 2012, 3, 2517−2522

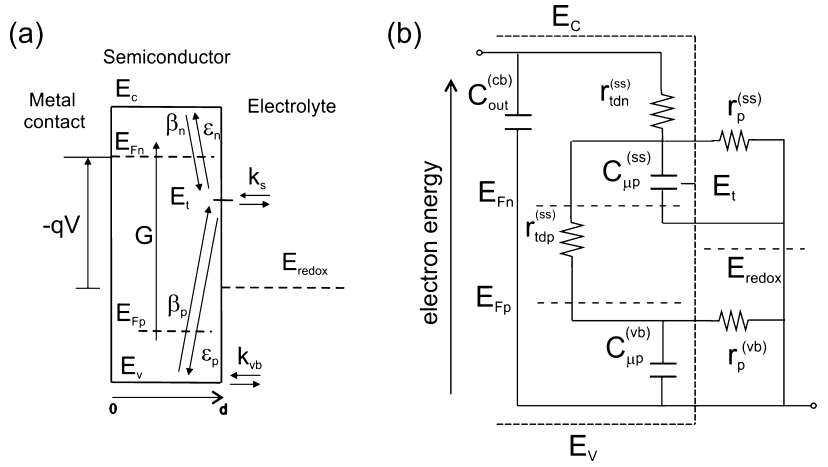

Figure 1. (a) Scheme of the kinetics of the processes occurring at the semiconductor/solution interface: generation of electrons and holes at a rate G, trapping of electrons from the conduction band (kinetic constant β_n) and detrapping (ε_n), trapping of holes from the valence band (β_p) and detrapping (ε_p), and charge transfer of holes from the traps (k_s) and from the valence band (k_{vb}). (b) Equivalent circuit (EC) obtained from a small ac perturbation. C_{out}^{cb} is the semiconductor capacitance, $C_{\mu p}^{ss}$ is the trap chemical capacitance, $C_{\mu p}^{vb}$ is the valence band chemical capacitance, r_{tdn}^{ss} is the trapping/detrapping resistance of electrons from the conduction band, r_{tdp}^{ss} is the trapping/detrapping resistance of holes from the valence band, r_p^{ss} is the charge-transfer resistance from the traps, and r_p^{vb} is hole's transfer resistance from the valence band.

On the other hand, the hole's quasi Fermi level (E_{Fp}) is *not* connected to the Fermi level of the metal contact, and holes can be created only by photogeneration, not by voltage injection.[20] We also assume the generation rate $G(x) = \alpha\phi_0 \exp(-\alpha x)$ at a fixed wavelength and given photon flux ϕ_0 and absorption coefficient α of the material. As the considered layer is very small (i.e., $d \ll \alpha^{-1}$), one can assume the layer to be quasi homogeneous so that n, p, and f can be considered uniform over the layer.[21] This model is simplified in the sense that the depletion layer and other internal structure conditions have been omitted in order to focus on the essential kinetic points, which are considered in detail as follows.

Two types of kinetic processes are shown in Figure 1a, (i) trap-assisted recombination of electrons, consisting of electron trapping (with kinetic constant β_n) and electron detrapping (ε_n) and holes trapping (β_p) and detrapping (ε_p), and (ii) charge transfer of holes from the traps (k_s) and from the valence band (k_{vb}). Clearly, for the fuel production purpose, the desired sense of carrier flux is the holes toward solution (anodic current), while the electron trapping induces recombination and is deleterious.

One can write the continuity equations for electrons and holes, neglecting hole diffusion, along with the master equation for traps that governs the trap's occupancy[21] as follows

$$\frac{\partial n}{\partial t} = -\frac{1}{q}\frac{\partial j_n}{\partial x} + G - \beta_n(1-f)nN_t + \varepsilon_n f N_t \tag{2}$$

$$\frac{\partial p}{\partial t} = G - \beta_p f p N_t + \varepsilon_p(1-f)N_t - k_{vb}(p - p_0) \tag{3}$$

$$\frac{\partial f}{\partial t} = \beta_n(1-f)n - \varepsilon_n f - \beta_p f p + \varepsilon_p(1-f) - k_s(f - f_0) \tag{4}$$

where q is the elementary charge.

At equilibrium, detailed balance leads to the useful relation

$$\frac{\varepsilon_n}{\beta_n n_0} = \frac{\beta_p p_0}{\varepsilon_p} = \exp\left(\frac{E_t - E_{F0}}{kT}\right) \tag{5}$$

We consider that the interface semiconductor/electrolyte is a blocking layer for electrons, which imposes that $j_n(d) = 0$. From this set of equations, the carrier densities and electrical current density at the cathode and in steady-state conditions (i.e., $\partial n/\partial t = 0$, $\partial p/\partial t = 0$, $\partial f/\partial t = 0$) can be calculated with the results

$$f = \frac{\beta_n \overline{n} + \varepsilon_p + k_s f_0}{\beta_n \overline{n} + \varepsilon_n + \beta_p \overline{p} + \varepsilon_p + k_s} \tag{6}$$

$$\overline{p} = \frac{G + \varepsilon_p(1-\overline{f})N_t + k_{vb}p_0}{\beta_p \overline{f} N_t + k_{vb}} \tag{7}$$

$$j = qd\left[G - \frac{\beta_n\beta_p N_t(\overline{n}\,\overline{p} - n_0 p_0)}{\beta_n \overline{n} + \varepsilon_n + \beta_p \overline{p} + \varepsilon_p + k_s} - \frac{\beta_n \varepsilon_n k_s N_t(\overline{n} - n_0)}{(\beta_n \overline{n} + \varepsilon_n + \beta_p \overline{p} + \varepsilon_p + k_s)(\beta_n \overline{n}_0 + \varepsilon_n)}\right] \tag{8}$$

where $\overline{x}$ corresponds to a steady-state quantity.

Examples of current density−voltage (j−V) curve are given in Figure 2 and are characterized by a voltage threshold because it is necessary to remove electrons from the traps in order to allow for a sizable rate of hole transfer to solution, first from the surface states and then from the valence band. Two main cases are distinguished, (a) $k_s \gg \varepsilon_n$ (curves 1 and 2), that is, easier hole transfer from the traps than electron trapping/detrapping, and (b) $k_s \ll \varepsilon_n$ (curves 3 and 4). For each of these cases, two subcases are shown, namely, $\beta_p \gg \beta_n$ (curves 2 and 4), that is, easier hole trapping/detrapping than electron trapping/detrapping, and $\beta_p \ll \beta_n$ (curves 1 and 3). From these plots, one can infer that the competition between electron trapping/detrapping and hole transfer from the traps has a more drastic influence on the j−V curve than that between electron and hole trapping/detrapping. Indeed, if ε_n increases with respect to k_s, there is a significant shift of the onset voltage. On the other hand, a relative change of β values has a minor effect on the curves. That is why we should focus on the ratio ε_n/k_s. However, the j−V plots do not provide a quantitative method

dx.doi.org/10.1021/jz3010909 | J. Phys. Chem. Lett. 2012, 3, 2517−2522

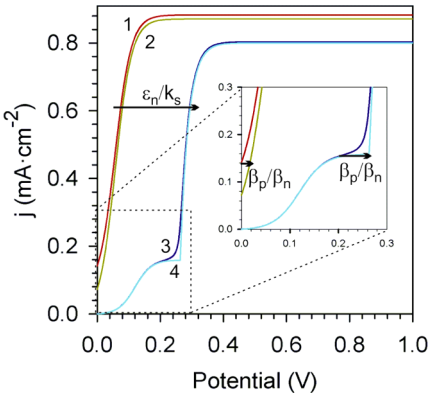

Figure 2. Current−voltage curves for different cases of the kinetic model including the electron trapping/detrapping, hole transfer from the trap, and hole trapping/detrapping. Model parameters are d = 10 nm, α^{-1} = 100 nm, $\phi_0 = 5 \times 10^{16}$ cm^{-2} s^{-1}, k_BT = 0.026 eV, E_c = 0 eV, E_t = −0.12 eV, $N_c = 10^{20}$ cm^{-3}, $N_t = 10^{21}$ cm^{-3}, and $k_{vb} = 10^{-1}$ s^{-1} (1), $\varepsilon_n = 10^{-1}/k_s = 1$ s^{-1}, $\beta_p = 10^{-3}/\beta_n = 10^{-21}$ cm^3 s^{-1} (2), $\varepsilon_n = 10^{-1}/k_s = 1$ s^{-1}, $\beta_p = 10^{3}/\beta_n = 10^{-15}$ cm^3 s^{-1} (3), $\varepsilon_n = 10^{3}/k_s = 10^{3}$ s^{-1}, $\beta_p = 10^{-3}/\beta_n = 10^{-18}$ cm^3 s^{-1} (4), $\varepsilon_n = 10^{3}/k_s = 10^{3}$ s^{-1}, $\beta_p = 10^{3}/\beta_n = 10^{-12}$ cm^3 s^{-1} .

to extract the values of k_s and ε_n. For this reason, the complex impedance of the system was then calculated.

The IS response of a system is usually characterized by an equivalent circuit (EC) consisting of resistors and capacitors. Here, we aim to obtain the impedance model from the detailed kinetic model that has been formulated above.

It is useful to introduce a number of quantities that appear in this type of calculation, mainly the chemical capacitances and charge-transfer resistances. The chemical capacitance is defined by the perturbation of charge in a given electronic state with respect to the thermodynamic potential.[22,23] In the present system, we can define three different equilibrium chemical capacitances, for the conduction band

$$C_\mu^{cb} = qd\frac{\partial \overline{n}}{\partial V} = \frac{q^2 d}{kT}\overline{n} \tag{9}$$

for the traps

$$C_{\mu eq}^{ss} = qdN_t\frac{\partial \overline{f}}{\partial V} = \frac{q^2 dN_t}{kT}(1-\overline{f})\left[\overline{f} - \frac{\varepsilon_p + k_s f_0}{\beta_n \overline{n} + \varepsilon_n + \beta_p \overline{p} + \varepsilon_p + k_s}\right] \tag{10}$$

and for the valence band

$$C_{\mu eq}^{vb} = qd\frac{\partial \overline{p}}{\partial V} = \frac{\beta_p \overline{p} + \varepsilon_p}{\beta_p N_t \overline{f} + k_{vb}} C_{\mu eq}^{ss} \tag{11}$$

The equilibrium chemical capacitance of traps is a quantity that has been often used for characterization of semiconductor surfaces.[24−26] For an n-type semiconductor under dark conditions (i.e., no holes) and at negative voltage, the capacitance in eq 10 takes the well-known form[21,23]

$$C_{\mu eq}^{ss} = N_t\frac{q^2 d}{kT}\overline{f}(1-\overline{f}) \tag{12}$$

It should also be remarked that the steady-state hole capacitance $C_{\mu eq}^{vb}$ in eq 11 explicitly depends on the chemical capacitance of the traps. This is due to the fact that holes in the valence band are not connected to any of the external Fermi levels, neither the Fermi level of the metal contact nor the redox level in solution (that contacts the counterelectrode). The population of holes in the valence band is governed by the kinetic processes of generation, recombination, and charge transfer and is affected by the voltage only through the change of electron density that modifies recombination, in our model.

We also introduce steady-state recombination resistances from the traps and from the valence band, defined respectively as

$$r_{rec}^{ss} = \frac{1}{k_s C_{\mu eq}^{ss}} \tag{13}$$

$$r_{rec}^{vb} = \frac{1}{k_{vb} C_{\mu eq}^{vb}} \tag{14}$$

The calculation of the impedance of our system is made by adding a small AC perturbation to the voltage, $V = \overline{V} + \tilde{V}\exp(j\omega t)$, that induces a small perturbation of the electron density that leads to $n = \overline{n} + \tilde{n}\exp(j\omega t)$, and similarly for the perturbation of the trap's occupation probability and the density of holes. From the resulting set of equations and applying the Laplace transform, the following complex admittance is obtained

$$Y = \frac{\tilde{j}_n(0)}{\tilde{V}} = j\omega C_\mu^{cb} + \left[r_{tdn}^{ss} + \frac{1}{j\omega C_{\mu p}^{ss} + (r_p^{ss})^{-1} + \frac{1}{r_{tdp}^{ss} + \frac{1}{j\omega C_{\mu p}^{vb} + (r_p^{vb})^{-1}}}}\right]^{-1} \tag{15}$$

In eq 15, we have introduced some capacitances that differ from the equilibrium values that were defined above. We have $C_{\mu p}^{ss}$, the chemical capacitance of the traps

$$C_{\mu p}^{ss} = B^{-1} C_{\mu eq}^{ss} \tag{16}$$

with

$$B = 1 - \frac{\beta_p \overline{p} + \varepsilon_p + k_s}{\beta_n \overline{n} + \varepsilon_n + \beta_p \overline{p} + \varepsilon_p + k_s} \tag{17}$$

$C_{\mu p}^{vb}$ is the capacitance of the valence band

$$C_{\mu p}^{vb} = B^{-1}\left(1 + \frac{k_{vb}}{\beta_p \overline{f} N_t}\right) C_{\mu eq}^{vb} \tag{18}$$

r_{tdn}^{ss} is the trapping/detrapping resistance of electrons that go from the conduction band to the traps (and vice versa)

$$r_{tdn}^{ss} = \frac{1}{(\beta_n \overline{n} + \varepsilon_n) C_{\mu p}^{ss}} \tag{19}$$

r_{tdp}^{ss} is the trapping/detrapping resistance of holes that go from the valence band to the traps (and vice versa)

$$r_{tdp}^{ss} = \frac{1}{(\beta_p \overline{p} + \varepsilon_p) C_{\mu p}^{ss}} \tag{20}$$

r_p^{ss} is the charge-transfer resistance from the traps

dx.doi.org/10.1021/jz3010909 | J. Phys. Chem. Lett. 2012, 3, 2517−2522

$$r_p^{ss} = B r_{rec}^{ss} \tag{21}$$

r_p^{vb} is the valence band hole transfer resistance

$$r_p^{vb} = B\left(1 + \frac{k_{vb}}{\beta_p \bar{f} N_t}\right)^{-1} r_{rec}^{vb} \tag{22}$$

In eq 15, the coupling of the impedance to the external voltage is regulated by the chemical capacitance of free electrons in the conduction band, C_μ^{cb}. In principle, it should be necessary to describe the electrostatic capacitances that are likely to be present in a real experiment, namely, the semiconductor capacitance due to the depletion layer C^{sc} and the Helmholtz capacitance. In order to take into account these effects, the outer capacitance is termed C_{out}^{cb} in Figure 1b. More rigorous calculations of C_{out}^{cb} must describe the specific morphology and the properties of the semiconductor surface, catalysts, and electrolyte, and such details are beyond the scope of this Letter.

Taking into account the expression of the admittance given by eq 15 and the generalized capacitance C_{out}^{cb}, the equivalent electrical circuit of Figure 1b was deduced. To our knowledge, this is the first equivalent AC circuit that models the kinetics of both electron and hole trap-assisted recombination and charge transfer at the semiconductor/electrolyte interface in the dynamic regime including explicitly the *three* chemical capacitances that are associated with the separated modes of carrier storage in this system, the conduction band, the valence band, and the surface states.

We discuss the main features of the EC to interpret the experimental IS spectra. While normally the models for this system predict the appearance of two arcs,[11,13] we remark that the EC of Figure 1b could, under some conditions, display three arcs, as shown by the example of Figure 3, one for the electron trapping/detrapping, another for the trap charge transfer, and one for the valence band charge transfer.

Experimentally, IS spectra usually reveal the existence of a maximum of two arcs observed at voltages corresponding to an optimum charge transfer from the traps.[18,19] At those voltages, the holes transfer from the valence band is much less probable than the transfer from the traps, and $r_p^{ss} \ll r_p^{vb}$. Consequently, because r_{tdp}^{ss} is in series with the parallel association of r_p^{vb} and $C_{\mu p}^{vb}$, the branch of the EC that contains r_p^{vb} and r_{tdp}^{ss} will not be observable at those voltages, and the EC in this case is the one given in Figure 4a. That is why a maximum of two semicircles is generally observed experimentally. However, if the holes Fermi level is taken to be sufficiently close to the valence band and if the charge transfer is dominated by the valence band states, it should be possible to observe the arc associated with the chemical capacitance of the valence band $C_{\mu p}^{vb}$. In fact, in silicon solar cells, it is feasible to observe both chemical capacitances for electrons and holes in the respective bands.[27]

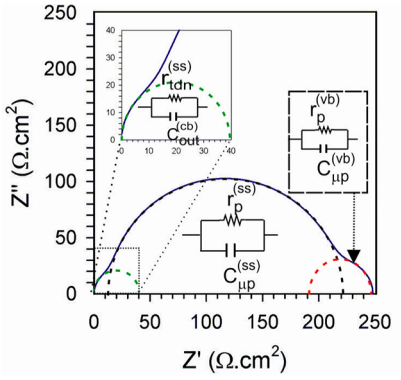

Figure 3. Illustration of the impedance in the complex plane presenting three semicircles. The first semicircle at low frequency corresponds to the valence band charge transfer, the second one corresponds to the surface state charge transfer, and the last one at higher frequencies corresponds to the electron trapping/detrapping. The parameters used for this simulation are d = 10 nm, α^{-1} = 100 nm, $\phi_0 = 5 \times 10^{16}$ cm^{-2} s^{-1}, kT = 0.026 eV, $N_c = 10^{20}$ cm^{-3}, $N_t = 10^{21}$ cm^{-3}, E_c = 0 eV, E_{F0} = 0 eV, E_t = 0 eV, $N_t = 2 \times 10^{21}$ cm^{-3}, $\varepsilon_n = 10^2$ s^{-1}, $\beta_n = 10^{-18}$ cm^3 s^{-1}, $\varepsilon_p = 5 \times 10^{-18}$ s^{-1}, $\beta_p = 2 \times 10^{-21}$ cm^3 s^{-1}, k_s = 10 s^{-1}, and k_{vb} = 0.7 s^{-1}.

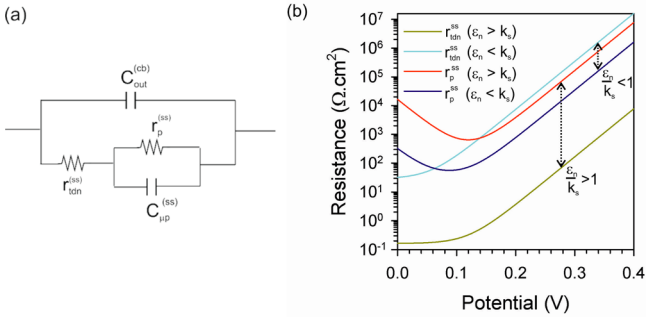

Figure 4. (a) EC for the case of low voltages. (b) Evolution of the resistances and capacitances involved in the EC of (a) as a function of voltage in the case of the current−voltage plots 2 and 3 of Figure 2.

An illustration is given in Figure 5a and b for the cases of the $j-V$ curves 2 and 3 of Figure 2. In Figure 5a, two arcs can be distinctly observed at 0.04 and 0.08 V. The first arc at lower frequencies corresponds to the charge transfer from the traps, while the semicircle at higher frequencies corresponds to the electron trapping/detrapping. Consequently, in the presence of those two semicircles, the recombination resistance r_{tdn}^{ss} and transfer resistance r_p^{ss} can be obtained. In the case of Figure 5b, only one semicircle can be observed. Because this IS spectrum corresponds to the $j-V$ curve 3 (i.e., $k_s \ll \varepsilon_n$), this semicircle corresponds to r_p^{ss}. The knowledge of r_p^{ss} and r_{tdn}^{ss} is sufficient to assess the quality of the semiconductor/solution interface because, as mentioned previously, the hole trapping/detrapping does not have a significant influence on the $j-V$ curves.

In order to deduce directly the kinetic parameter out of the values of both resistances, the ratio r_{tdn}^{ss}/r_p^{ss} can be calculated using eqs 1, 5, 19, and 21.

$$\frac{r_{tdn}^{ss}}{r_p^{ss}} = \frac{k_s}{(\beta_n \bar{n} + \varepsilon_n)} = \gamma(V) \times \frac{k_s}{\varepsilon_n} \tag{23}$$

where

$$\gamma(V) = \left[1 + \exp\left(\frac{E_{F0} - E_t}{kT}\right)\exp\left(-\frac{qV}{kT}\right)\right]^{-1} \tag{24}$$

From eq 24, one can notice that the relative value of r_{tdn}^{ss} and r_p^{ss} depends, as expected, on the rate of charge transfer (k_s) and recombination (ε_n) but also on a factor γ determined by the voltage and the trap depth, which takes values between 0 and 1. At zero voltage, γ depends exclusively on the trap depth in the band gap. As the voltage increases, $\exp(-V/k_BT) \to 0$ and $\gamma \to 1$. Depending on the difference between k_s and ε_n, the relative

dx.doi.org/10.1021/jz3010909 | J. Phys. Chem. Lett. 2012, 3, 2517−2522

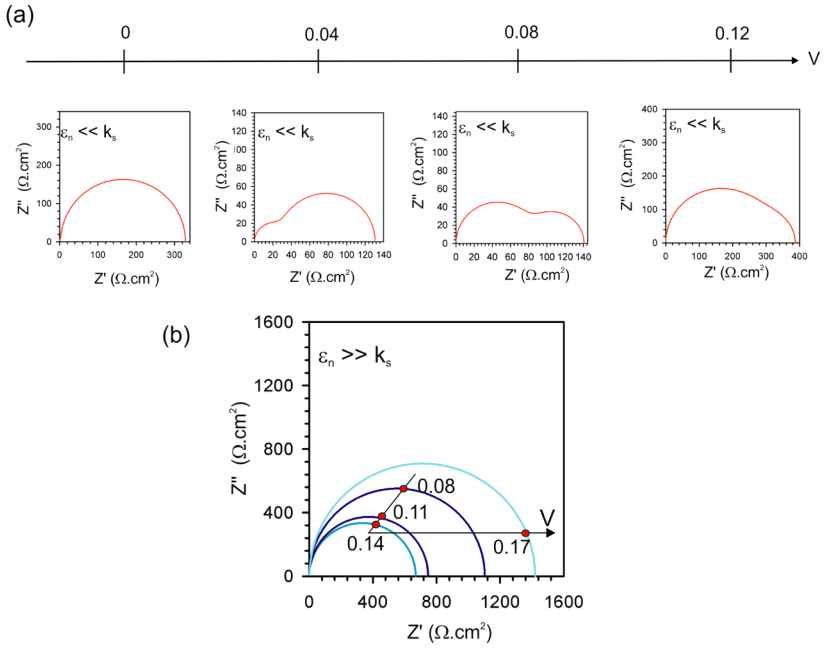

Figure 5. Evolution of the impedance spectra obtained by IS in the case of (a) the $j-V$ curve 2 of Figure 2 (i.e., $\varepsilon_n = 10^{-1}/k_s = 1\ s^{-1}$, $\beta_p = 10^3/\beta_n = 10^{-15}\ cm^3\ s^{-1}$) and (b) the $j-V$ curve 3 of Figure 2 (i.e., $\varepsilon_n = 10^3/k_s = 10^3\ s^{-1}$, $\beta_p = 10^{-3}/\beta_n = 10^{-18}\ cm^3\ s^{-1}$).

values of r_{tdn}^{ss} and r_p^{ss} can therefore evolve with voltage (see Figure 4b), inducing a possible variation of the relative size of both semicircles as for Figure 5a.

In conclusion, we have proposed an EC that models the kinetics of the interface semiconductor/electrolyte in water splitting conditions taking into account electrons and holes. The main important new feature of this circuit is that we provide a rigorous structure of the fundamental EC for water splitting systems with all of the physically necessary elements, including the charge-transfer resistance and the capacitance of the valence band, which should be observed if the holes quasi Fermi level is taken to be close to the valence band. Moreover, this EC allows for the determination of the main physical processes that limit the current density at lower positive voltage, electrons recombination and charge transfer from the traps.

AUTHOR INFORMATION

Corresponding Author

*E-mail: bisquert@uji.es.

Notes

The authors declare no competing financial interest.

ACKNOWLEDGMENTS

We thank financial support from Explora Sup Rhône Alpes, Ministerio de Ciencia e Innovación under Project HOPE CSD2007-00007, and Generalitat Valenciana (Projects ISIC/2012/008 "Institute of Nanotechnologies for Clean Energies" and PROMETEO/2009/058).

REFERENCES

(1) Bolts, J. M.; Wrighton, M. S. Correlation of Photocurrent–Voltage Curves with Flat-Band Potential for Stable Photoelectrodes for the Photoelectrolysis of Water. *J. Phys. Chem.* **1976**, *80*, 2641–2645.

(2) Butler, M. A.; Ginley, D. S. Principles of Photoelectrochemical, Solar Energy Conversion. *J. Mater. Sci.* **1980**, *15*, 1–19.

(3) Walter, M. G.; Warren, E. L.; McKone, J. R.; Boettcher, S. W.; Mi, Q.; Santori, E. A.; Lewis, N. S. Solar Water Splitting Cells. *Chem. Rev.* **2010**, *110*, 6446–6473.

(4) Nocera, D. G. The Artificial Leaf. *Acc. Chem. Res.* **2012**, *45*, 767–776.

(5) Bjoerksten, U.; Moser, J.; Graetzel, M. Photoelectrochemical Studies on Nanocrystalline Hematite Films. *Chem. Mater.* **1994**, *6*, 858–863.

(6) Lin, Y.; Yuan, G.; Sheehan, S.; Zhou, S.; Wang, D. Hematite-Based Solar Water Splitting: Challenges and Opportunities. *Energy Environ. Sci.* **2011**, *4*, 4862.

(7) Mayer, M. T.; Du, C.; Wang, D. Hematite/Si Nanowire Dual-Absorber System for Photoelectrochemical Water Splitting at Low Applied Potentials. *J. Am. Chem. Soc.* **2012**, *134*, 12406–12409.

(8) Katz, M. J.; Riha, S. C.; Jeong, N. C.; Martinson, A. B. F.; Farha, O. K.; Hupp, J. T. Toward Solar Fuels: Water Splitting with Sunlight and Rust? *Coord. Chem. Rev.* **2012**, DOI: dx.doi.org/10.1016/j.ccr.2012.06.017.

(9) Klahr, B. M.; Hamann, T. W. Current and Voltage Limiting Processes in Thin Film Hematite Electrodes. *J. Phys. Chem. C* **2011**, *115*, 8393–8399.

(10) Vanmaekelbergh, D.; Cardon, F. Calculation of the Electrical Impedance Associated with the Surface Recombination of Free Carriers at an Illuminated Semiconductor/Electrolyte Interface. *J. Phys. D: Appl. Phys.* **1986**, *19*, 643.

(11) Ponomarev, E. A.; Peter, L. M. A. Comparison of Intensity Modulated Photocurrent Spectroscopy and Photoelectrochemical Impedance Spectroscopy in a Study of Photoelectrochemical Hydrogen Evolution at p-InP. *J. Electroanal. Chem.* **1995**, *397*, 45–52.

(12) Hens, Z. The Electrochemical Impedance on One-Equivalent Electrode Processes at Dark Semiconductor Redox Electrodes Involving Charge Transfer through Surface States. 1. Theory. *J. Phys. Chem. B* **1999**, *103*, 122–129.

(13) Leng, W. H.; Zhang, Z.; Zhang, J. Q.; Cao, C. N. Investigation of the Kinetics of a TiO_2 Photoelectrocatalytic Reaction Involving Charge Transfer and Recombination through Surface States by Electrochemical Impedance Spectroscopy. *J. Phys. Chem. B* **2005**, *109*, 15008–15023.

(14) Wijayanthaa, K. G. U.; Saremi-Yarahmadia, S.; Peter, L. M. Kinetics of Oxygen Evolution at α-Fe_2O_3 Photoanodes: a Study by

Photoelectrochemical Impedance Spectroscopy. *Phys. Chem. Chem. Phys.* **2010**, *13*, 5264−5270.
(15) Zhong, D. K.; Gamelin, D. R. Photoelectrochemical Water Oxidation by Cobalt Catalyst ("Co−Pi")/α-Fe_2O_3 Composite Photoanodes: Oxygen Evolution and Resolution of a Kinetic Bottleneck. *J. Am. Chem. Soc.* **2010**, *132*, 4202−4207.
(16) Barroso, M.; Mesa, C. A.; Pendlebury, S. R.; Cowan, A. J.; Hisatomi, T.; Sivula, K.; Gratzel, M.; Klug, D. R.; Durrant, J. R. Dynamics of Photogenerated Holes in Surface Modified Fe_2O_3 Photoanodes for Solar Water Splitting. *Proc. Natl. Acad. Sci. U.S.A.* **2012**, DOI: 10.1073/pnas.1118326109.
(17) Klahr, B.; Gimenez, S.; Fabregat-Santiago, F.; Hamann, T.; Bisquert, J. Water Oxidation at Hematite Photoelectrodes: The Role of Surface States. *J. Am. Chem. Soc.* **2012**, *134*, 4294−4302.
(18) Klahr, B.; Gimenez, S.; Fabregat-Santiago, F.; Bisquert, J.; Hamann, T. W. Electrochemical and Photoelectrochemical Investigation of Water Oxidation with Hematite Electrodes. *Energy Environ. Sci.* **2012**, *5*, 7626−7636.
(19) Braun, A.; Sivula, K.; Bora, D. K.; Zhu, J.; Zhang, L.; Grätzel, M.; Guo, J.; Constable, E. C. Direct Observation of Two Electron Holes in a Hematite Photoanode During Photoelectrochemical Water Splitting. *J. Phys. Chem. C* **2012**, *116*, 16870−16875.
(20) Salvador, P. Semiconductors' Photoelectrochemistry: A Kinetic and Thermodynamic Analysis in the Light of Equilibrium and Nonequilibrium Models. *J. Phys. Chem. B* **2001**, *105*, 6128−6141.
(21) Bisquert, J. Theory of the Impedance of Charge Transfer via Surface States in Dye-Sensitized Solar Cells. *J. Electroanal. Chem.* **2010**, *646*, 43−51.
(22) Bisquert, J. Chemical Capacitance of Nanostructured Semiconductors: its Origin and Significance for Heterogeneous Solar Cells. *Phys. Chem. Chem. Phys.* **2003**, *5*, 5360−5364.
(23) Bisquert, J. Beyond The Quasi-Static Approximation: Impedance and Capacitance of an Exponential Distribution of Traps. *Phys. Rev. B* **2008**, *77*, 235203.
(24) Frese, K. W.; Morrison, S. R. Electrochemical Measurements of Interface States at the GaAs/Oxide Interface. *J. Electrochem. Soc.* **1979**, *126*, 1235−1241.
(25) Dare-Edwards, M. P.; Hamnett, A.; Trevellick, P. R. Alternating-Current Techniques in Semiconductor Electrochemistry. *J. Chem. Soc., Faraday Trans. 1* **1983**, *79*, 2111−2124.
(26) Allongue, P.; Cachet, H. I−V Curve and Surface State Capacitance at Illuminated Semiconductor/Liquid Contacts. *J. Electroanal. Chem.* **1984**, *176*, 369−375.
(27) Mora-Seró, I.; Luo, Y.; Garcia-Belmonte, G.; Bisquert, J.; Muñoz, D.; Voz, C.; Puigdollers, J.; Alcubilla, R. Recombination Rates in Heterojunction Silicon Solar Cells Analyzed by Impedance Spectroscopy at Forward Bias and under Illumination. *Energy Mater. Solar Cells* **2008**, *92*, 505−509.